JETIR.ORG

JOURNAL OF EMERGING TECHNOLOGIES AND



INNOVATIVE RESEARCH (JETIR)

An International Scholarly Open Access, Peer-reviewed, Refereed Journal

CHEF-BASED OPTIMIZATION ALGORITHM (CBOA)-BASED GLOBAL PEAK POWER MONITORING SYSTEM FOR PHOTOVOLTAIC SYSTEMS

¹ Syed Shahid Afridh ² M.Sreenivasulu

^{1,2} Department of Electrical and Electronics Engineering

^{1,2} Gokula Krishna College of Engineering

ABSTRACT: The need for clean and renewable energy sources is being driven by environmental concerns. Photovoltaic (PV) systems have seen a remarkable increase in use among renewable energy sources in recent decades. Temperature, shadow percentage, and insolation are just a few of the variables that impact how well the PV system operates. Due to changes in isolation and temperature, the intermediate converter between the solar panels and the load modifies the voltage differential between the PV output and the load. Natural or artificial shading of the solar panel results in many peaks in the P-V, which causes technical problems, qualities. While the other peaks are categorized as Local Peak Power (LPP), one of the several peaks is known as Global Peak Power (GPP). It is challenging to determine GPP throughout the optimization process due to the existence of several peaks and the potential for trapping at LPP rather than GPP. In order to track the GPP of the PV system, this study introduces the Chef-based Optimization Algorithm (CBOA). Compared to Particle Swarm Optimization (PSO) and Grey Wolf Optimization (GWO), CBOA offers a more structured method. It was designed based on the process of learning cooking skills in training classes. The execution of Using a 5S5P setup, the tracking algorithm is simulated in MATLAB. In the simulation simulations, the CBOA outperforms PSO and GWO in terms of tracking time and maximum power magnitude

INDEX TERMS: Local peak power (LPP), global peak power (GPP), photovoltaic (PV) systems, and chef-based optimization algorithms (CBOA).

I. INTRODUCTION The demand for energy is rising dramatically every day in every nation due to increased industry and population growth [1]. In view of future demand and environmental concerns, many nations have passed legislation mandating a significant use of natural resources in power generation in order to attain Net Zero Pollution (NZP) [2]. Solar energy, which is also utilized to produce electricity, is one of the most popular natural resources [3]. PV systems convert solar energy into usable electrical energy [4]. Temperature, shade percentage, and insolation all affect how the PV system operates [5]. The converter between the solar panels and the load regulates the insufficiency of PV output power due to temperature and insolation [6]. Shadowing on the solar panel caused by natural or artificial processes results in several peaks in the P-V characteristics, which leads to numerous technical issues [7].

While the other peaks are classified as Local Peak Power (LPP), one of the several summits has real Global Peak Power (GPP) [8].to produce GPP by adjusting the intermediate dc-dc converter duty cycle (δ) in line with PV voltage

and current [9]. Tracking controllers can be broadly classified into three categories: conventional, intelligent, and optimization methods [10]. These methods differ in their operating ranges and hardware implementation convergence times [11]. Among the conventional and optimization methods found in the literature are Perturb & Observe [12], Hill Climbing [13], Incremental Conductance [14], Genetic Algorithm [15], Particle Swarm Optimization Cuckoo Search Adaptive Jaya and Spotted Hyena Optimization. Conventional tracking techniques are still widely used for efficient tracking in uniform insolation, but they function at LPP in shaded environments, leading to low efficiency and lengthy tracking times. Optimization strategies are more reliable than traditional methods even if the population number considered for the system is the same in all operational scenarios In their evaluation of tracking methods, K at che et al. divided them into three categories: traditional, intelligent, and hybrid. Following an evaluation of various methods based on factors including tracking speed, practical viability, and efficiency, a performance hierarchy was developed. In order to improve global MPPT (GMPPT) under partial shade conditions, Bhukya et al. added an extra stage to the traditional Perturb and Observe (P&O) algorithm. Ali and associates. For grid-integrated PV systems, suggested a fuzzy logic controller (FLC) to guarantee steady voltage output while resolving uncertainties and disruptions related to reactive power and DC link voltage regulation. An artificial neural network (ANN)-based MPPT technique was created in to efficiently track the global power point for a grid-connected photovoltaic system using a multilayer inverter under dynamically changing weather circumstances, therefore lowering overall harmonic distortion. Basha and associates, introduced a hybrid GMPPT method that combined an adaptive neuro-fuzzy inference system (ANFIS) with a modified GWO. Using open-circuit voltage (VOC) and peak power point voltage (VPP) restrictions to achieve accurate and quick tracking, the modified GWO algorithm was used to optimize the ANFIS's membership functions. However, delays in the ANFIS feedback signal limit the PV system's performance to some extent.

In order to monitor the GPP under partial shade circumstances (PSC), Wang and Sun presented a hybrid tracking P&O algorithm with technique that combines a backstepping control. Although the controller performed dependably in straightforward designs, it found it difficult to reliably handle problems in more intricate system architectures. A thorough analysis of MPPT schemes was provided in [2], classifying them according to their procedural approaches and comparing their effectiveness in terms of tracking speed and efficiency. To properly integrate maximum power into the grid, a low-cost photovoltaic (PV) converter is still needed. Priyadarshini and associates. For standalone PV systems, developed a hybrid MPPT technique that combines model predictive control (MPC) and discrete integral sliding mode control (DISMC). The suggested controller produced quick computational response while successfully reducing steady-state faults. In, a honey bee dance algorithm was used to harvest maximum power under situations of varying solar irradiation. To enable accurate MPPT in PV systems exposed to partial shading, Demirci et al. combined an artificial neural network (ANN) with a metaheuristic algorithm.

For global peak power point tracking (GPPT) in PV systems, the Chef-Based Optimization Algorithm (CBOA) has a number of advantages over traditional metaheuristic algorithms like PSO and GWO. A more balanced exploration and exploitation of the search space is made possible by CBOA's structured learning mechanism, which is inspired by culinary training, in contrast to PSO, which relies on velocity and position updates that frequently lead to premature convergence and entrapment in local optima.

This methodical approach improves tracking accuracy by increasing adaptation to changing insolation patterns and dynamic shading circumstances. With its multi-stage learning approach, CBOA successfully diversifies the search process in contrast to GWO, which mimics the social hierarchy of grey wolves but frequently shows delayed convergence in complicated, multimodal search landscapes. This feature makes it possible for CBOA to more effectively avoid local peak points (LPP), guaranteeing reliable tracking of the global peak point (GPP) even in extremely non-uniform insolation conditions. Additionally, by striking the ideal balance between convergence speed and tracking accuracy, CBOA demonstrates improved computing efficiency while drastically lowering steady-state oscillations and power losses. These benefits make CBOA a viable substitute for improving MPPT's dependability

and effectiveness in PV systems running in actual environmental settings. Table 1 shows a comparison of CBOA with current algorithms. Thus, the implementation of the CBOA tracking method for the 5S5P configuration is presented in this work

The paper is organized as follows: Section II covers the PV system under PSC. Volume 13, 2025; CBOA algorithm 156247 A. Jain and associates: Global Peak Power Monitoring System for Photovoltaic Systems Based on CBOA Figure 1: The PV system's schematic diagram is described in Section III. Section IV displays the outcomes of the simulation. Section V concludes the paper. The schematic diagram of the PV system is shown in Figure 1.

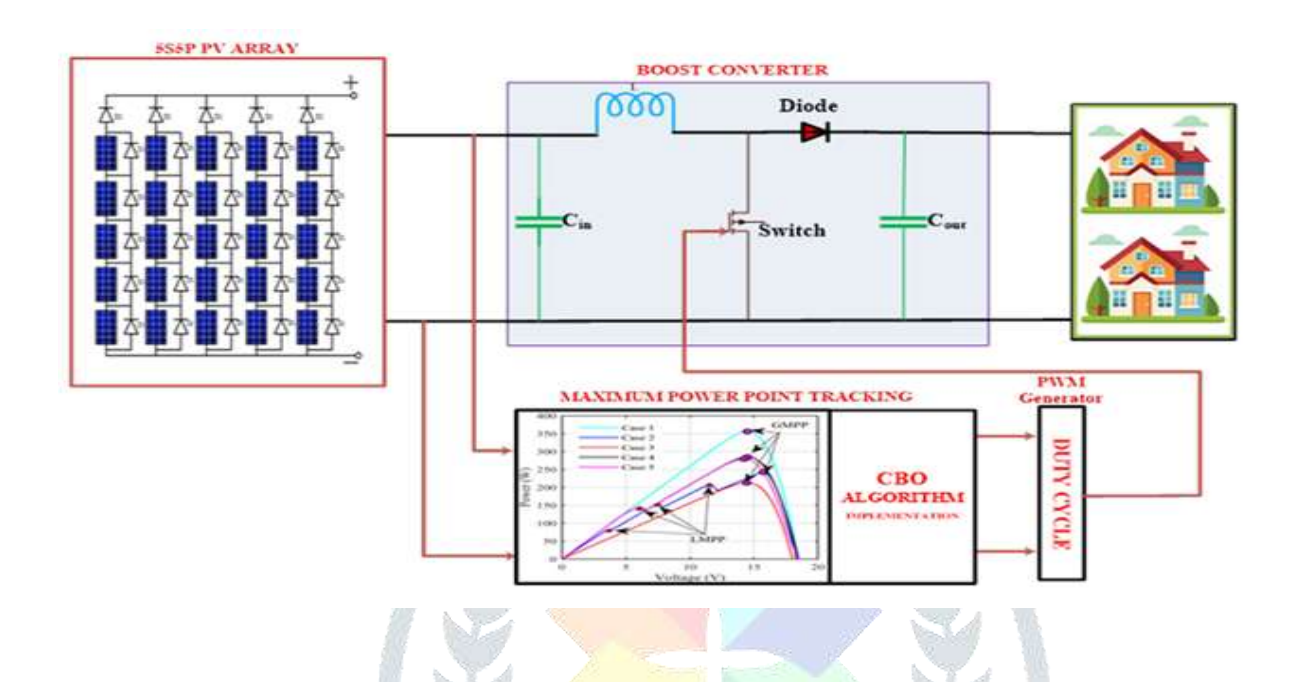


FIGURE 1: Schematic diagram of PV system.

II. PSC'S PV SYSTEM: Usually placed on rooftops, photovoltaic (PV) modules are subject to a variety of environmental conditions. Obstacles including passing clouds, shadows from nearby structures, dust accumulation, and bird droppings often make it impossible to provide uniform irradiance throughout the entire array. This state, known as PSC, is inevitable throughout the production of solar power. PSC can physically damage the panels, leading to the formation of hot spots, in addition to lowering the overall performance of the PV system. To reduce this type of damage, bypass diodes are commonly employed with PV modules. PV modules connected in parallel show mismatched currents, whereas those connected in series experience uneven voltages under PSC. The system's power-voltage (P-V) characteristics show several peaks when operating under PSC with bypass diodes. The Global Peak Point (GPP) is the peak with the largest magnitude among them; the other peaks are referred to as local peaks.

The PV module's effective insolation decreases under PSC. Equation 1 provides the effective insolation (GE) for each shaded PV module.

$$G_E = (1 - S)G \tag{1}$$

where G is the insolation of the PV module and Sis is the shading ratio of the panel. The shading ratio is the proportion of the module's shaded area to its total area. Equations 2, 3, and 4 at the foot of the following page provide generalized mathematical equations for the output current and voltage of a PV array with "n" number of PV modules during PSC. where BK is Boltzman's constant, RS is series resistance,

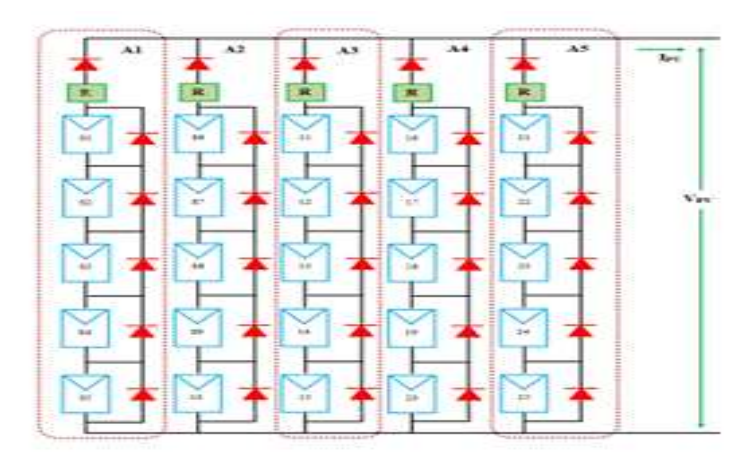


FIGURE 2. 5S5PconfigurationofthePVsystem

A is the diode ideality factor, and NS is the number of PV cells. Equations 2 and 3 represent the output current of the (n-1) and (n-2) PV modules, respectively, as IPh(n-1) and IPh(n-2). Unshaded PV modules continue to function at optimal efficiency under PSC. Because of the constant current f low throughout the string, shaded PV modules in a series configuration become reverse-biased yet still need to carry the same current as the unshaded modules. This opposite polarity causes the shaded cells to use power instead of producing it, which reduces the total output power of the PV system. In severe circumstances, an excessive amount of reverse voltage may result in the formation of hotspots or even an open circuit throughout the PV string. Bypass diodes are installed in PV modules to prevent this type of damage.

These diodes allow the shaded modules to be avoided by providing a different path for current flow during shading. Consequently, shaded and unshaded modules have different currents. Bypass diodes increase the output power of the PV system under PSC, but they also result in several peaks in the P-V characteristics.

Table 2 displays the AP-PM-15PV panel's electrical specs. Fig. 2 depicts the schematic diagram of the 5S5P (five-series, five-parallel) structure, with several coloring conditions described in Table 3. Figure 3 displays the matching computed P-V and I-V characteristics for different shading scenarios.

if
$$I_{PV} > I_{Ph}(n-1)$$

$$I_{PV} = I_{Ph}(G_n) - I_D \left[\exp\left(\frac{q(V_{PVmn} + I_{PV}R_S)}{N_S A B_K T}\right) - 1 \right] - \frac{V_{PVmn} + I_{PV}R_S N_S}{N_S R_{Sh}} V_{PV} = V_{PV(n-1)}$$
(2)

if
$$I_{Ph}(n-2) < I_{Pv} > I_{Ph}(n-1)$$

$$I_{PV} = I_{Ph}(G_n - 1) - I_D \left[\exp\left(\frac{q(V_{PVm(n-1)} + I_{PV}R_S)}{N_SAB_KT}\right) - 1\right] - \frac{V_{PVm(n-1)} + I_{PV}R_SN_S}{N_SR_{Sh}} V_{PV}$$

$$= V_{PV(n-1)} (2)$$
(3)

 $if I_{PV} > I_{Ph1}$

$$I_{PV} = I_{Ph}(G_1) - I_D \left[\exp\left(\frac{q(V_{PVml} + I_{PV}R_S)}{N_S A B_K T}\right) - 1 \right] - \frac{V_{PVml} + I_{PV}R_S N_S}{N_S R_{Sh}} V_{PV}$$

$$V_{PV} = V_{PV1} + V_{PV(n-1)} \dots \dots + V_{PV1}$$
(4)

It is evident from Fig. 3 that the PSConPV setup results in several peaks. The configuration's output power is lowered to different numerical values due to shading on the 5S5PPV panels. The PV output power, voltage, and current at GPP for Case 1, or uniform isolation, are 373.6W, 85.256V, and 4.38A, respectively. Four peaks are produced in the curve in Case 2 because symmetrical shading is applied to the PV arrangement. LPP values are (161.6W,70.8787V and 2.2801A), (138.42W,55.8804V and 2.4771A), and (98.5W,33.2714V and 2.9607A), respectively.

GPP values are 169W,91.1155V and 1.8544A. The LPP values at Case 3 are (154.2W, 71.0166V and 2.1717A), (129.8W, 51.7381V and 2.5084A), and (93.2264W, 32.9793V and 2.8268A). The GPP values are 158.7712W, 91.8770V and 1.7281A).

The PV arrangement in Cases 4 and 5 is subjected to random insolation levels, which causes the characteristics to display several peaks. GPP (167.44W, 90.8032V and 1.8440A) and LPP (161.14W, 70.6156V and 2.2819A), (137.05W, 53.7380V and 2.5504A), and (100.1461W, 35.3189V and 2.8341A) for Case 4 and GPP (193.6W, 90.2841A) and LPP (175.6349W, 76.1358V and 2.3069A).

III. CHEF-BASE DOPTIMIZATIONAL METHOD (CBOA)

The training course for mastering cooking skills is the source of inspiration for CBOA's computational operations. The trainees are modeled using the matrix shown in equation 5 below.

$$Y = \begin{bmatrix} Y_1 \\ \vdots \\ Y_i \\ \vdots \\ Y_{N} \end{bmatrix} = \begin{bmatrix} y_{1,1} & \dots & y_{1,j} & \dots & y_{1,m} \\ \vdots & \ddots & \vdots & \ddots & \vdots \\ y_{i,1} & \dots & y_{i,j} & \dots & y_{i,m} \\ \vdots & \ddots & \vdots & \ddots & \vdots \\ y_{N,1} & \dots & y_{N,j} & \dots & y_{N,N} \end{bmatrix}$$
 (5)

where Y is the matrix's population, Yi is the ith member/candidate solution, yi,j is the jth problem variable of ith candidates' answer, N is the total number of members, or population size, and m is the number of variables. During the first phase of implementation, the position of the CBOA members is randomly started, and members are generated at random using Eq. (6).

$$y_{i,j} = LB_j + r.\left(UB_j - LB_j\right) \tag{6}$$

where UB_i and LB_i are the lower and upper bounds for the jth issue variable, and r is a random number generated using the normal distribution function. The objective function is evaluated for each CBO member using the function definition, and the evaluated function values are stored in a vector (F). Equation 7 represents the values of the objective function.

$$Y = \begin{bmatrix} F_1 \\ \vdots \\ F_i \\ \vdots \\ F_N \end{bmatrix} = \begin{bmatrix} F(Y_1) \\ \vdots \\ F(Y_i) \\ \vdots \\ F(Y_N) \end{bmatrix}$$

$$(7)$$

where Fi is the objective function determined for each member of the CBOA. Following the assessment of the initial population's objective function values, the CBOA is used to improve

the potential fixes. The population is first divided into two groups by the algorithm: cookery students and instructing chefs. Different tactics are used to update members' positions within and between these groups.

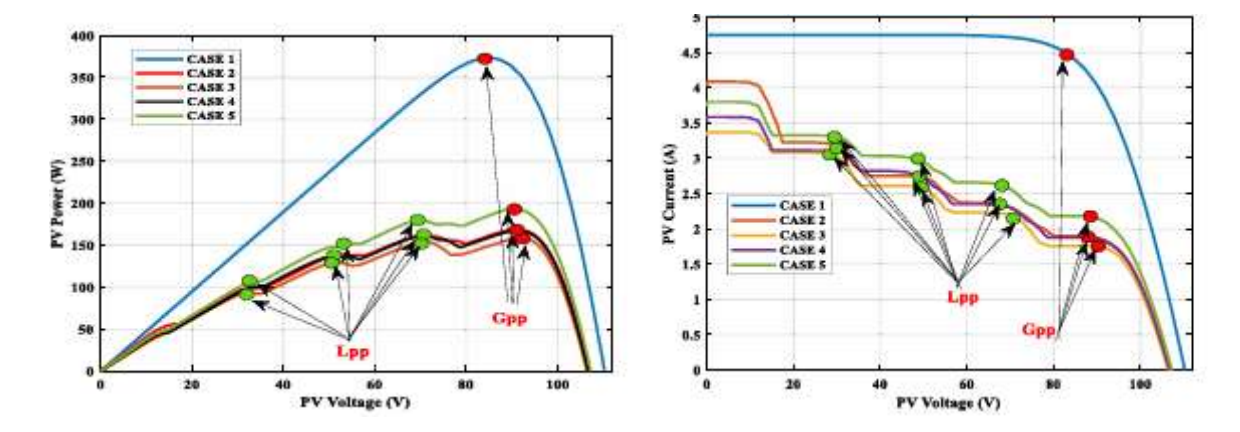


FIGURE 3 (a) P-V and I-V characteristics of 5S5Pconfiguration

All members' objective function values are evaluated, and the best performers are chosen to serve as chef teachers to direct further iterations. in equations 8 and 9.

$$XS = \begin{bmatrix} XS_1 \\ \vdots \\ XS_{NC} \\ XS_{NC+1} \\ \vdots \\ XS_N \end{bmatrix} = \begin{bmatrix} xs_{1,1} & \dots & xs_{1,j} & \dots & xs_{1,m} \\ \vdots & \ddots & \vdots & \ddots & \vdots \\ xs_{NC,1} & \dots & xs_{NC,j} & \dots & xs_{NC,m} \\ xs_{NC+1} & \dots & xs_{NC+1,j} & \dots & xs_{NC+1,m} \\ \vdots & \ddots & \vdots & \ddots & \vdots \\ xs_{N,1} & \dots & xs_{N,j} & \dots & xs_{N,N} \end{bmatrix}$$
(8)

where XS is a sorted matrix, with XS1 to XSNC representing the members of the instructors' group and XSNC+1 to XSN representing the members of the cookery students' group. FSisavector of sorted objective function. Now, let's say that vector FSi has objective function values that correspond to XS1 to XSN.

Two distinct approaches are used to update the new position of the chief teachers. In the first strategy, new roles are calculated using equation 10 and reorganized according on the best chef position.

$$FS = \begin{bmatrix} FS_1 \\ \vdots \\ FS_{NC} \\ FS_{NC+1} \\ \vdots \\ FS_N \end{bmatrix}$$

$$(9)$$

The second category's technique is centered on location-based search and exploitation since it is more likely to produce better results. A local search

$$XS_{ij}^{C/S1} = xs_{i,j} + r.(BC_j - I.xs_{i,j})$$
(10)

$$XS_i = \begin{cases} XS_i^{C/S1} & , FS_i^{C/S1} < F_i \\ XS_i & else \end{cases} \tag{11}$$

Space is created around the positions of each chief instructor. Equations 12 and 13 allow for controlled exploration within a – size parameters.

where LBlocal j and UBlocal j are the jth local problem variables.

$$LB_j^{Local} = \frac{LB_j}{t} \tag{12}$$

$$UB_j^{Local} = \frac{UB_j}{t} \tag{13}$$

t is the current iteration number, and lower and upper bounds, respectively. Local boundaries are used to construct (14)). new

$$XS_{ij}^{C/S2} = xs_{i,j} + LB_j^{Local} + r.\left(UB_j^{Local} - LB_j^{Local}\right) \quad (14)$$

In this case, j = 1,2,3... mandi =

1,2.... NC. The constraint for updating an existing position is implemented using equation 15, where xsC/S2 i,j is the jth coordinate of a member, FSC/S2 i is the objective function value of the member for updated position, and XSC/S2 i is the newly evaluated position for the ith sorted member (i.e., XSi) based on the Second Strategy (C/S2) of Chef instructors updating process.

$$XS_i = \begin{cases} XS_i^{C/S2} & , FS_i^{C/S2} < F_i; \\ XS_i & else \end{cases}$$
 (15)

The role of chief teachers is changed in method 1 to enhance their abilities prior to instructing their students. Therefore, this approach reflects the global search and exploration capabilities of CBOA and keeps the algorithm from becoming trapped in

local maximums. Each main instructor in strategy 2 strives to enhance his culinary abilities through personal practice.

This tactic demonstrates the algorithm's capacity for local search and exploitation. A non-linear, smoother transition between exploration and exploitation is guaranteed by the cosine function. To prevent local optima, random scaling introduces variation.

Following the updating of the chef teacher position, three distinct methodologies are also used to update the cooking student position.

Strategy 1: Every pupil must receive training from a chief instructor in order to develop new abilities. Each student's new position is updated depending on the instructor's random choice for

$$XS_{i,i}^{S/S1} = xs_{i,i} + r.(CI_{ki,i} - I.xs_{ki,i})$$
(16)

rategy 1, XSS/S1 i is the new position evaluated for the first member of the sorted matrix (i.e., XSi). (S/S1) of the process of updating the position of cooking appliances, xsS/S1 i,j is jth coordinate, and CIki,j is a randomly selected chef trainer by a culinary student, where CIki, i signifies the magnitude xski, i and ki is arbitrarily selected from the set{1,2,3,..,NC}.

The former position is updated following a successful improvement in the objective function. Equation (17) models this limitation for

$$XS_{i} = \begin{cases} XS_{i}^{S/S1} & , FS_{i}^{S/S1} < F_{i}; \\ XS_{i} & else \end{cases}$$
 (17)

where the objective function value for XSS/S1 i is FSS/S1 i.

Strategy 2: In this phase, each apprentice works with the chef instructor to imitate the instructor's style. The instructor chooses the talent to train at random from the vector of skills. This idea is applied mathematically to update the cooking student's position by using Equation (18)

$$XS_i = \begin{cases} CI_{ki,j} & , j = 1\\ XS_{i,j} & else \end{cases}$$
 (18)

When a better objective function value is obtained by using equation 19, it instantly switches with the old one. XSi = XSS/S2 i,FSS/S2 i <Fi; XSi,else (19), where xsS/S2 i,j is the jth coordinate, FSS/S2 i is the magnitude of the objective function, and XSS/S2 i is the new estimated position based on method 2 (S/S2) of updating the location of cooking apprentice for the ithmember of sortedmatrix (i.e., XSi).

$$XS_i = \begin{cases} XS_i^{S/S2} & , FS_i^{S/S2} < F_i; \\ XS_i & else \end{cases}$$
 (19)

Strategy 3: Using local search and exploitation, each apprentice works to improve their cooking skills through personal hobbies and workouts.tion. The bound for the local search space is produced using

Equations (6) and (7). Equation (20) is used to determine a cookery student's new position.

$$XS_{ij}^{S/S3} = \begin{cases} xs_{i,j} + LB_j^{Local} + r. \left(UB_j^{Local} - LB_j^{Local} \right) & ,j = q \\ xs_{i,j} & ,j \neq q \end{cases}$$
(20)

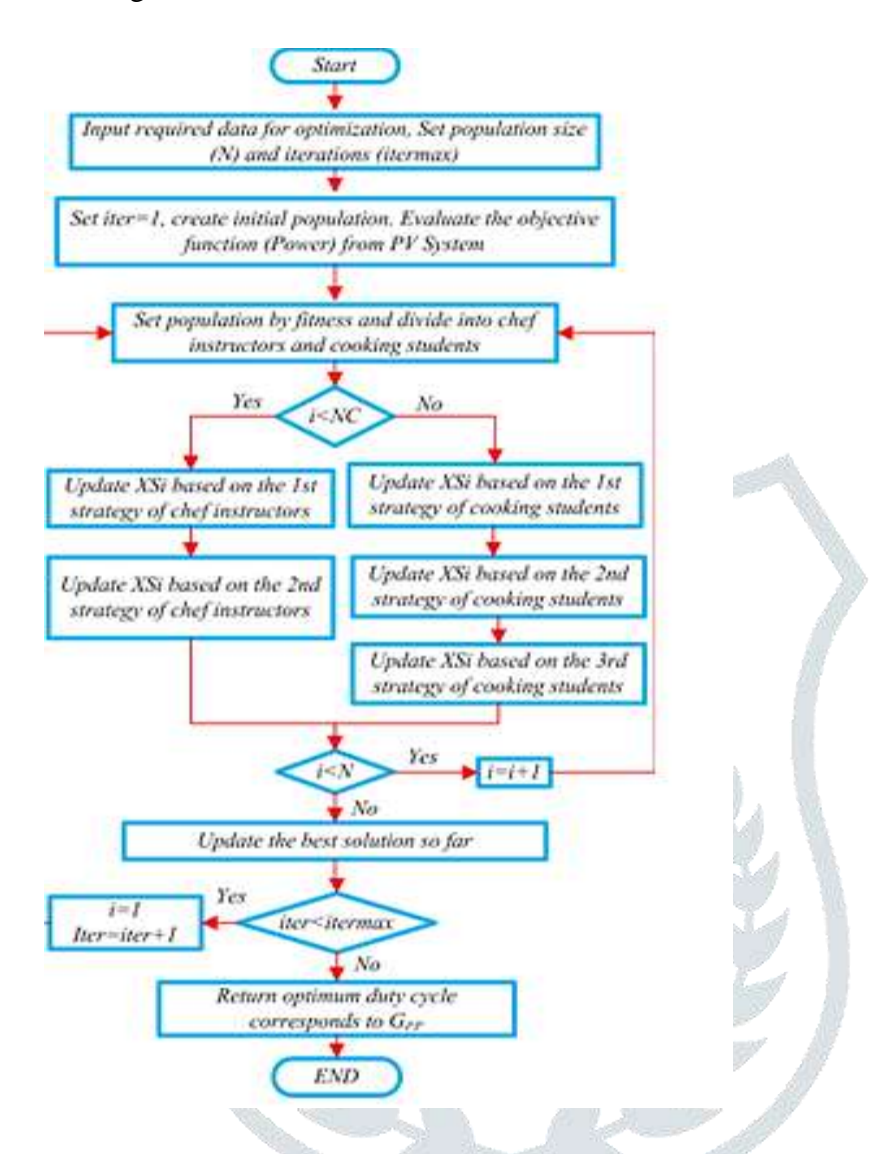
is the new evaluated magnitude for the ith member of CBOA of sorted matrix (that is, XSi) based on strategy 3 (S/S3) of updating position of cooking apprentices, and q is a random number chosen from the set

$$XS_{i} = \begin{cases} XS_{i}^{S/S3}, FS_{i}^{S/S3} < F_{i} \\ XS_{i} & else \end{cases}$$
 (21)

where the objective function value for XSS/S3 i (21) is FSS/S3 i, FSS/S3 i, otherwise <Fi>. Every iteration uses Equations (6) and (21) to update the positions of all participants in the training and instruction process with a uniform structure. The CBOA algorithm's f lowchart is shown in Fig. 4. IV. DISCUSSIONS AND RESULTS

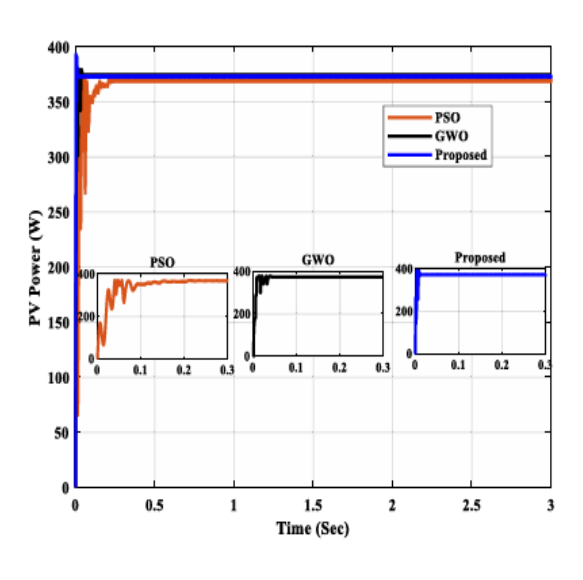
First, a simulation study utilizing PSO, GWO, and the suggested CBOA algorithm is conducted on 5S5P configuration. use the MATLAB 2024a ode45 solver with Ts = 1 ms for accuracy and compatibility. Cin = 100µF. L = 10mH, Cout = 330 µF, and MOSFET as the switching device are the simulation parameters for the boost converter. Component values were selected using typical design trade-offs for stability. To enable comparison on a consistent platform, all three methods are simulated using the same parameters. The metrics used to compare the tracking methods' performance are actual obtained power (P obtained), efficiency ($\eta = (P \text{ obtained} / PActual) \times$ 100%), voltage, and current. Five distinct instances are used to assess the simulation study. Case 1: In this scenario, the 5S5P structure receives uniform insolation at a temperature of 250C, or 1000 W/m2. Following simulation, it is noted that the PSO

A maximum power of 367.3W has been retrieved by the algorithm. Similarly, 368.7W of electricity is extracted via GWO. The maximum power of 372.5W is produced by the suggested algorithm, which differs very little from the actual power obtained, as Fig. 5



Consequently, the proposed approach outperforms PSO and GWO. The voltage and current readings are 79.26V, 4.634A, 80.81V, 4.562A, and 83.03V, 4.486A. GWO, PSO. order. for and the suggested method, in that Case 2: As shown in Table 3, the PV system is simulated under PSC with a 100 W/m2 insolation differential between each panel. Consequently, the PV system has produced a maximum power of 168.96W because of the shading pattern. Similar to the previous example, the suggested CBOA method tracked the GPP in 0.025 seconds to extract 167.9W.

Whereas, the PSO and GWO has reached an optimal power 163.2Wand165.5Wwithinatrackingtimeof0.12secand 0.07 sec correspondingly as shown in Fig.6. Case 3: The proposed CBOA algorithm demonstrates its superiority in the GPP tracking by achieving a power output remarkably close to the actual maximum power obtained. In this case, the actual power recorded is 158.7W, and the proposed method effectively extracts 157.7W,



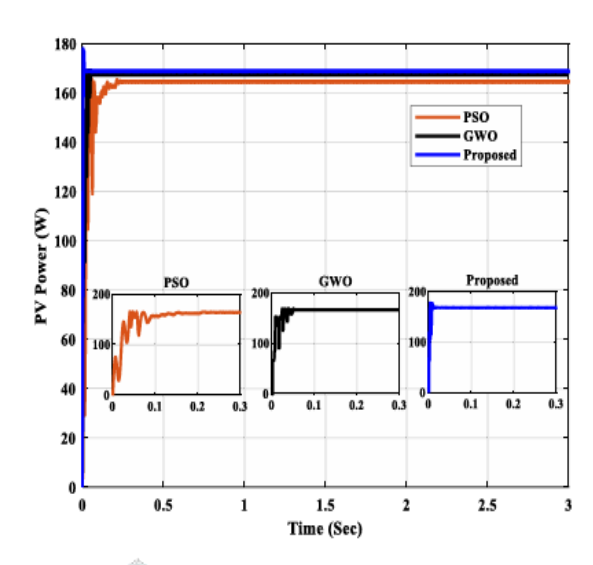


FIGURE 5. PV system output power using PSO, FIGURE 6. PV System Output Power using PSO, GWO and CBOA algorithm under case 1 GWO and CBOA algorithm under case 2

demonstrating its great tracking effectiveness. Nevertheless, GWO and PSO algorithms produce photovoltaic (PV) power outputs of 154.5 W and 153.4 W, respectively. which, as shown in Fig. 6, are less than the output produced by the suggested strategy. This demonstrates how well the suggested algorithm tracks the GPP in a variety of environmental circumstances. Its accuracy and resilience are demonstrated by the output's closer alignment with the real maximum power.

V. CONCLUSION:

The current work proposes a novel metaheuristic technique called the chef-based optimization algorithm to maximize power from PV arrays under PSC. The recommended The method is compared with PSO and GWO and evaluated for five different PSC scenarios. Simulation findings validate the benefit of the proposed method in terms of maximum power, tracking speed, and steady state oscillations. Table 6 reports optimization findings utilizing parameters such as mean, standard deviation, median, and execution time.

- CASE1: Compared to PSO at 367.3W and GWO at 368.7W, the suggested method has produced the maximum power of 372.5W.
- CASE2: The suggested technique takes 0.025 seconds to extract maximum power, while PSO and GWO attain optimal power in 0.12 seconds. and 0.07 seconds, in that order.
- CASE3: In this instance, the suggested algorithm outperforms PSO and GWO in precisely and effectively tracking the GPP.
- .CASE 4: In just 0.0188 seconds, the suggested technique produces 166.2 W that is closer to the real output power peak value.

.CASE5: Among the four peaks, the suggested CBOA tracks the GPP more effectively than PSO and GWO. Compared to PSO at 98.31% and GWO at 98.92%, the suggested method is effective and easy to execute, delivering maximum power with 99.67% efficiency.

REFERENCES:

- [1] H. Gundogdu, A. Demirci, S. M. Tercan, and U. Cali, "A novel improved global maximum power point tracker method based on the grey wolf algorithm" IEEE Access, vol. 12, pp. 6148–6159, 2024, doi: 10.1109/ACCESS.2024.3350269, "considering partial shading."
- [2] "A quick and effective MPPT scheme for solar power generation during dynamic weather and partial shaded conditions," by M. N. Bhukya and V. R. Kota Eng. Sci. Technol., Int. J., vol. 22, no. 3, pp. 869–884, June 2019, doi:

10.1016/j.jestch.2019.01.015.

- [3] "Optimal planning and designing of microgrid systems with hybrid renewable energy technologies for sustainable environment in cities," by P. Kurukuri, M. R. Mohamed, P. H. Raavi, and Y. Arya Environmental Science and Pollution Research, vol. 31, no. 22, pp. 1–18, April 2024
- [4] A. K. Bansal, V. S. Sangtani, and M. N. Bhukya, "Optimal configuration and sensitivity analysis of hybrid nanogrid for futuristic residential application using honey badger algorithm," Energy Convers. Manage., vol. 315,Art. No. 118784, September 2024.
- [5] S. Vunnam, M. Vanitha Sri, and R. Alla, "An outline of solar photovoltaic systems impact on environment," Bull. Electr. Eng. Informat., vol. 12, no. 5, pp. 2635–2642, Oct. 2023.
- [6] G. H. Reddy, S. R. Depuru, S. Gope, B. V. Narayana, and M. N. Bhukya, "Multiple rooftop solar PV integrated electric vehicle charging stations placed simultaneously for reliability benefits," IEEE Access, vol. 11, pp. 130788–130801, 2023.
- [7] I. Sajid, A. Gautam, A. Sarwar, M. Tariq, H.-D. Liu, S. Ahmad, C.-H. Lin, and A. E. Sayed, "Using dandelion optimizer (DO)-based MPPT to optimize photovoltaic power production in partial shading conditions" approach," Processes, vol. 11, no. 8, p. 2493, Aug. 2023.
- [8] V. R. Kota and M. N. Bhukya, "A novel global MPP tracking scheme based on shading pattern identification using artificial neural networks for photovoltaic (PV) power generation during partial shaded condition," IET Renew. Power Generat., vol. 13, no. 10, pp. 1647–1659, July 2019.
- [9] IET Renew. Power Gener., vol. 14, no. 9, pp. 1433–1452, 2020; R. B. Bollipo, S. Mikkili, and P. K. Bonthagorla, "Critical review on PV MPPT techniques: Classical, intelligent and optimization."
- [10] S. Arandhakar, N. Chaudhary, S. R. Depuru, R. K. Dubey, and M. N. Bhukya, "Analysis and implementation of robust Metaheuristic algorithm to extract essential parameters of solar cell," IEEE Access, volume 10, pages 40079–40092, 2022.
- [11] O. Boubaker, "MPPT techniques for photovoltaic systems: A systematic review in current trends and recent advances in artificial intelligence," Discover Energy, vol. 3, no. 1, p. 9, 2023.
- [12] G. A. Raiker, U. Loganathan, and S. B. Reddy, "Current control of boost converter for PV interface with momentum-based perturb and observe MPPT," IEEE Trans. Ind. Appl., vol. 57, no. 4, pp. 4071–4079, July 2021, doi: 10.1109/TIA.2021.3081519.
- [13] V. Kumar and M. Singh, "Derated mode of power generation in PV system using modified perturb and observe MPPT algorithm," J. Mod. Power Syst. Clean Energy, vol. 9, no. 5, pp. 1183–1192, Sep. 2021, doi: 10.35833/mpce.2019.000258.
- [14]. Eskandarian, and S. Mobayen, "Improvement of self-predictive incremental conductance algorithm with the ability to detect dynamic conditions," Energies, vol. 14, no. 5, p. 1234, February 2021.
- [15] A. Borni, T. Abdelkrim, N. Bouarroudj, A. Bouchakour, L. Zaghba, A. Lakhdari, and L. Zarour, "Optimized MPPT controllers using GA for grid connected photovoltaic systems, comparative study," Energy Proc., vol. 119, pp. 278–296, July 2017.